Acta Cryst. (1977). A**33**, 412–418

Dynamical Contrast of the Topographic Image of a Crystal with Continuous X-ray Radiation. I. An Experimental Observation of Polychromatic Interference Fringes and their Application for the Investigation of the Anomalous Scattering of X-rays by Perfect Crystals*

BY V. V. ARISTOV, I. M. SHMYTKO AND E. V. SHULAKOV

Solid State Physics Institute, Academy of Sciences of the USSR, Moskovskaya Oblast, Chernogolovka, 142432, *USSR*

(*Received* 31 *March* 1976; *accepted* 13 *December* 1976)

Contrast is investigated of topographic images obtained on perfect plane-parallel and wedge-shaped crystals with continuous X-ray radiation. Quasiperiodic variation of intensity was observed on the topographs of plane-parallel wafers in the direction of the change of wavelength. It is experimentally shown that these oscillations of intensity are interference fringes. An analysis is given of the formation of polychromatic interference fringes from wedge-shaped wafers. A method is suggested on the basis of this analysis for determining the atomic scattering factor over a wide range of wavelengths. The method was used for the determination of atomic scattering factors of Si and Ge. The phenomenon of anomalous scattering at the K absorption edge of Ge was experimentally observed.

I. Introduction

Interest in the development of new methods and in the investigation of schemes involving diffraction of continuous X-ray radiation by a crystal arises because these methods are simple, fast and do not require special instrumentation. Recently, we have investigated the contrast of topographic images obtained from a block crystal with continuous radiation, and demonstrated that such topographs enable one to measure with high accuracy the angles between blocks (Aristov & Shulakov, 1975). By studying the contrast on topographs obtained with continuous radiation for a transmission arrangement (Laue diffraction) from plane-parallel wafers, cut from perfect Si crystals, we found a quasiperiodic variation of intensity in the direction of the change of wavelength (Aristov, Shmytko & Shulakov, 1976*a*).

This paper presents the results of the experimental and theoretical investigation of the contrast of topographic images of plane-parallel and wedge-shaped Si and Ge crystals with continuous radiation. It is shown that the observed oscillations of intensity are interference fringes.† The principle of finding the dependence of the atomic scattering factor $f_{\mathbf{h}}$ on the wavelength of X-ray radiation is described.‡ This principle is based on measuring the fringe spacing on the topographs recorded with continuous radiation from the plane-parallel and wedge-shaped crystals.§. The results are given of measuring the atomic scattering factor $f_{\mathbf{h}}$ with the plane-parallel wafers for the 111 reflexion of Si over the short-wavelength range and with the wedge-shaped wafers for both the 220 reflexion of Si and the 111 reflexion of Ge over the wavelength range from 0·3 to 0·9 Å and from 0·9 to 1·4 Å respectively. The experimental results are compared with the theoretical dependences $f_{\mathbf{h}}(\lambda)$.

2. Experimental procedure

Fig. 1 presents the geometrical arrangement for obtaining the topographs. A point source of continuous X-ray radiation S is placed at the distance D_1 from the entrance surface of the investigated crystal. A slit 1 limits the beam divergence to 20° and serves to protect the film from exposure to the primary beam. The radiation diffracted by the crystal is focused on a line at the distance D_2 from the exit crystal surface.* The film is placed in parallel with the crystal surface at the distance D_2+D_3 from it. In order to decrease the background produced by radiation scattered by various elements of the set-up, a slit 2, $1-3$ mm wide, is placed at the distance D_2 from the crystal in the location of the focal spot of the diffracted rays.

* Copyright reserved by All-Union Agency on Authors' Rights.

† *Pendellösung* fringes for the diffraction of continuous radiation from wedge portions of Si single crystals were reported by Hashimoto, Kozaki & Ohkawa (1965) and Kozai, Ohkawa & Hashimoto (1968).

‡ We denote the atomic scattering factor for the value of (sin θ)/λ, corresponding to a reflexion *hkl*, by $f_{\mathbf{h}}$.

§ The method of determination of $f_{\mathbf{h}}$ from the measurements of *Pendellösung* fringe spacings with monochromatic radiation has advanced considerably in recent years (Kato, 1969; Pinsker, 1974). However, such measurements were possible only for the wavelengths λ of the characteristic emission of the several elements used as anodes in X-ray tubes. Recently, Fukamachi & Hosoya (1975) have described a method of determining $f_{\mathbf{h}}(\lambda)$ near the absorption edge for polar crystals, based on measuring the intensity of diffracted continuous radiation.

* We shall discuss only the symmetric Laue case, therefore $D_1=D_2$.

The experimental set-up was mounted on a microfocus X-ray generator Microflex. Ag and Au anodes were used for the production of intensive *bremsstrahlung* radiation. Focus dimensions did not exceed 20μm. The investigated perfect Si crystals were cut in the shape of plane-parallel wafers 0·3 – 1·5 mm thick and wedge-shaped wafers with angles from 1 to 4°. Ge crystals were cut in the shape of wedge-shaped wafers with an angle from 1 to 2°. All samples were prepared in such a manner that reflexions could be obtained from the planes normal to the specimen surface. The 111 and 220 reflexions were used.

Let us call the radial direction **OX** and the azimuthal direction **OY** (Fig. 1). As follows from the experimental geometry, the image of the crystal on the topograph is magnified $m_x = D_3/D_1$ times in the radial and $m_y = 2+(D_3/D_1)$ times in the azimuthal direction. For $D_3>0$ the image on the topograph is inverted. The exact value of the magnification factor is readily determined by comparing the crystal dimensions with those of its image.

In the experimental geometry discussed, images of different portions of a crystal are formed by different wavelengths. For the specimens with dimensions small in comparison with D_1 and at not too large diffraction angles we can assume with sufficient accuracy that the λ = constant curves are straight lines, parallel to the azimuthal direction, and that the wavelength of the diffracted wave varies only in the radial direction **OX**. We assume the point of intersection of the perpendicular to the crystal surface, drawn from the source *S*, with the film surface to be the origin of the coordinate system on the film. Then the wavelength λ, corresponding exactly to the Bragg equation $2d_{\mathbf{h}} \sin\theta = \lambda$, and the point on the film with coordinate *x*, on which this radiation is incident, are related by the formula:

$$x = D_3 \tan\theta = D_3\lambda(2d_{\mathbf{h}}\cos\theta)^{-1}. \qquad (1)$$

Normally the value of D_3 and particularly the position of the coordinate origin (of the point *O*) are known only approximately, so that in order to find the relation between the coordinate *x* and wavelength λ according to (1) we have to measure the positions of two characteristic lines on the film. The jumps of photoemulsion sensitivity at the Ag and Br *K* absorption edges, clearly seen on topographs, can be used for the same purpose.

3. Dynamical contrast of the topographic image of the plane-parallel wafer

It is known that the dynamical contrast of topographic images of monocrystals is defined by their degree of perfection and their thickness. For example, in obtaining the topographic images with a monochromatic plane wave from the wedge-shaped wafers, the changes of intensity are observed which are called *Pendellösung* fringes (Kato & Lang, 1959; Kato, 1961). In order to exclude the effect of a change in the crystal thickness on the contrast of topographic images, we first investigated the diffraction of continuous radiation by the plane-parallel Si crystals.

Fig. 2(*a*) illustrates a fragment of the topograph, obtained from a plane-parallel Si wafer 0·74 mm thick. The reflecting planes were (111), and the distances were $D_1 = D_2 = 5$ cm, $D_3 = 25$ cm. Gold-anode radiation was used. The figure reveals seven fringes, almost parallel to the azimuthal direction. In order to show that these fringes are connected only with the diffraction by a perfect crystal and are not caused by structural defects, we set the crystal in the same position as that in the case of Fig. 2(*a*), and scanned it during the exposure along **OX** in a plane parallel to the crystal surface. The interval of crystal scanning Δx_{cr} was 8 mm, for the fringe spacing on the topograph 1·4 mm. The film remained fixed. In this method of obtaining X-ray topographs each point of the film receives the rays diffracted from all points of the corresponding segment Δx_{cr} of the crystal, so that the topographic images of defects are blurred out (Aristov, Shmytko & Shulakov, 1976*b*). Fig. 2(*b*) gives a fragment of the scanning topograph, which shows the same fringes as in Fig. 2(*a*). The two topographs differ only in fringe contrast, which is due to the presence in the crystal of defects and to the surface roughnesses being imaged in a different manner in these two methods of recording topographs. Thus, we come to a conclusion that quasiperiodic variations of contrast are caused not by the crystal defect structure, but only by the change of wavelength along the radial direction.

Normally, the topographs recorded with continuous radiation showed characteristic radiation lines. Each line possesses a fine structure depending on whether the line is in the maximum or minimum of intensity of the fringes observed. Fig. 3 gives the distribution of intensity in the radial direction for the doublet of charac-

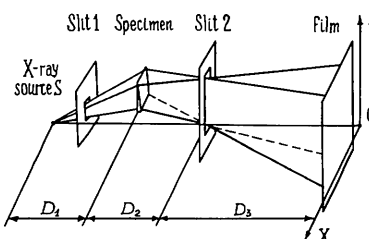

Fig. 1. Experimental arrangement. The crystal investigated is a plane-parallel wafer or wedge-shaped.

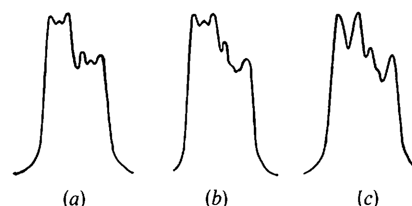

Fig. 3. Intensity distribution in the doublet of characteristic lines Ag $K\alpha_1$ and Ag $K\alpha_2$.

teristic lines Ag $K\alpha_1$ and Ag $K\alpha_2$. The distribution (*a*) corresponds to the case when both lines lie in the maximum of fringe intensity, (*b*) shows one of the intermediate positions and (*c*) corresponds to both lines located in the minimum of fringe intensity. The fine structure of the diffraction lines obtained from a point source is the result of interference of wave fields inside the crystal and is described by the dynamical theory of X-ray diffraction (Authier & Simon, 1968; Indenbom & Chukhovskii, 1972). The differences between the distributions of Fig. 3(*a*) and (*c*) demonstrate that the contrast on topographs is also of interference nature. Indeed, the intensity distributions, similar to those in Fig. 3, are repeated for each monochromatic wave. On the film these intensity distributions superpose with displacements relative to each other. In our experiments the distances between fringes are much greater than the width of the reflexion of a characteristic line, so that it can be assumed that the successive distinct portions of one and the same intensity distribution λ = constant, characteristic for a given point x, are summed at each point of the topograph. For instance, the distributions which superpose near the fringe maxima are of the type given in Fig. 3(*a*), and those which superpose near minima are of the type shown in Fig. 3(*c*). Therefore, it can be expected that the integral intensity on a topograph, obtained by superposition of almost identical intensity distributions for different wavelengths, is similar to the angular integral intensity, obtained in the case of the diffraction of a plane monochromatic wave by a perfect crystal (Waller, 1926).

According to the dynamical theory of X-ray diffraction, for $\mu t \ll 1$ (μ is the linear absorption coefficient), the expression for integral intensity under symmetric Laue diffraction is given by the equation (Zachariasen, 1945):

$$I_{\mathbf{h}} \sim \int_0^{2A} \mathscr{I}_0(\varrho)\mathrm{d}\varrho \tag{2.1}$$

$$A = KC|\chi_{\mathbf{h}}|t/2\cos\theta\,. \tag{2.2}$$

Here $K = 2\pi/\lambda$; $\chi_{\mathbf{h}}$ is the **h**th Fourier coefficient of polarizability of the crystal for X-rays, determined by the reciprocal-lattice vector for a given reflexion; C is the polarization factor, equal to 1 for the σ polarization and to $|\cos 2\theta|$ for the π polarization.* The maxima of the integral intensity are defined by the condition $2A = \varrho_{2l+1}$, where $l = 0, 1, 2\ldots$ and ϱ_{2l+1} are zeros of Bessel's function of zero order. For $l \geq 4$ it can be assumed that $\varrho_{2l+1} - \varrho_{2l-1} \simeq 2\pi$, hence the period of intensity oscillations is due to the change of the parameter A by π. Normally, *Pendellösung* fringes are obtained with monochromatic radiation from wedge-shaped wafers. In the case under discussion the crystal thickness is constant, but the wavelength varies in the radial direction. When λ varies, the value of A changes in the same way as in the case of variation of the thickness t. From (1) and the formula for A, it follows that if the fringes in Fig. 2 are of interference origin, their spacing Λ_x in the first approximation must be equal to

$$\Lambda_x = D_3(2d_{\mathbf{h}}Ct|\chi_{\mathbf{h}}|/\lambda^2)^{-1} - D_3 \tan\theta(|\chi_{\mathbf{h}}|/\lambda^2)^{-1}\Delta(|\chi_{\mathbf{h}}|/\lambda^2)\,. \tag{3}$$

The range of wavelengths used for recording topographs was 0·25 to 1·5 Å. The K absorption edge for Si is 6·74 Å, so that we can assume with sufficient accuracy that $|\chi_{\mathbf{h}}|/\lambda^2$ = constant over the whole topograph. This means that $\Delta(|\chi_{\mathbf{h}}|/\lambda^2) = 0$ and the fringe spacing must also be constant. The value of Λ_x enables one to find the amplitude of the structure factor $F_{\mathbf{h}}$, which is related to $|\chi_{\mathbf{h}}|$ by the equation:

$$|F_{\mathbf{h}}| = \pi\Omega(mc^2/e^2)(|\chi_{\mathbf{h}}|/\lambda^2) \tag{4.1}$$

where Ω is the unit-cell volume, m is the electron mass, c is the light velocity, and e is the electron charge. For a crystal containing one kind of atom, from $F_{\mathbf{h}}$ one can determine the atomic scattering factor by the expression:

$$F_{\mathbf{h}} = f_{\mathbf{h}} \sum_j \exp\left[2\pi i(hu_j + kv_j + lw_j)\right] \tag{4.2}$$

were u_j, v_j, w_j are the fractional coordinates of the centres of the atoms in the unit cell.

From the above it follows that in order to verify the assumption that the fringes observed are those of integral intensity appearing because of the change of λ, one should investigate the dependence of a number of fringes N and spacings Λ_x on different parameters and correlate these dependencies with those following from (3). Having recorded topographs of crystals of different thickness with varied experimental geometry, we have established that: (*a*) the number of fringes for constant geometrical arrangement is proportional to the crystal thickness t ($N \sim t, \Lambda_x \sim t^{-1}$); (*b*) for constant crystal thickness the number of fringes on the topograph changes only with changes in the distance D_1, and the number of fringes per fixed range of wavelengths remains constant; (*c*) The fringe spacing is nearly constant over the whole topograph, *i.e.* Λ_x is proportional to Δx and hence to the change of $\Delta\lambda/\cos\theta$; (*d*) fringes are observed only for small absorption, and vanish at $\mu t > 3$.

Thus, the experimental data obtained support the hypothesis concerning the character of contrast on topographs obtained with continuous radiation. Interference fringes observed are due to the oscillations of integral intensity in the direction of wavelength variation. This intensity is formed by superposition at each point of monochromatic intensity distributions, shifted with respect to one another; each such distribution has its own corresponding wavelength. Such a mechanism

* (2.2) determines the parameter A when the diffraction plane of X-rays is normal to the crystal surface. In the case under discussion, the diffraction plane rotates by an angle φ around the normal to the reflexion planes when the X-rays incident on the crystal deviate in the direction **OY**. The effect of azimuthal divergence has been analyzed by us in the following paper (Aristov, Shmytko & Shulakov, 1977) and it has been shown that a more exact value of the parameter A is $A = KC|\chi_{\mathbf{h}}|t/2\cos\theta\cos\varphi$, where $\tan\varphi = y/(2D_1 + D_3)$. In our experiments the φ value was less than 5°, so we shall assume below that $\cos\varphi \simeq 1$.

of forming the integral intensity differs from those considered earlier for monochromatic plane and spherical waves. For this reason we shall call the integral intensity, obtained with the X-ray continuous radiation, the polychromatic integral intensity.

4. Measurement of the atomic scattering factor on plane-parallel perfect crystal wafers

We now show that the use of continuous radiation makes it possible to determine the atomic scattering factor from the oscillation of integral intensity with varying wavelength. Let us analyse the factors affecting the accuracy of measuring $f_{\mathbf{h}}$. Fig. 4 represents the distribution of photodensity on the topograph whose fragment is shown in Fig. 2(*a*). The general shape of the curve is caused by the distribution of intensity over the wavelength, $\sigma(\lambda)$, of the radiation incident on the crystal, and by the dependence of photoemulsion sensitivity on wavelength. Thus, the short-wavelength segment of the curve corresponds to an increase of $\sigma(\lambda)$ as the wavelength rises from $\lambda_V = 12{\cdot}4/V \simeq 0{\cdot}25$ Å (V is the voltage applied to the X-ray tube, $V = 50$ kV) to $\lambda = \frac{3}{2}\lambda_V = 0{\cdot}4$ Å; the intensity jump at $\lambda = 0{\cdot}48$ Å corresponds to the K absorption edge of the silver incorporated into the photoemulsion composition. It is apparent that despite large variations of $\sigma(\lambda)$ and of photoemulsion sensitivity, the fringe contrast remains satisfactory up to $\lambda \simeq 0{\cdot}65$ Å. Over the range from $\lambda = 0{\cdot}65$ to $\lambda = 0{\cdot}8$ Å the contrast vanishes, and after the fading region, changes to the opposite contrast. This means that contrast changes are caused by the presence in the X-ray radiation of two states of polarization.* Calculations by means of the dynamical theory of X-ray diffraction (Aristov *et al.*, 1977) demonstrate that the first vanishing of contrast in the case under discussion should take place for $\lambda_e \simeq 0{\cdot}73$ Å. This value is in good agreement with the wavelength for which contrast fades away in Fig. 4. The presence of two states of polarization in the X-ray radiation changes the fringe spacing observed. Because of this, (3) gives a correct value of the fringe spacing which is observed in the experiment if the coefficient C is assigned to the value $0{\cdot}5(1 + |\cos 2\theta|)$ (Pinsker, 1974). On a topograph, shown in Fig. 2(*a*), the change of the fringe spacing due to the decrease of the coefficient C with increasing θ is less than 0·5%.

* The change of contrast, and of the *Pendellösung* fringe spacing observed with monochromatic rays, due to the presence in the X-ray radiation of two states of polarization has been investigated on wedge-shaped crystals by Hattori, Kuriyama & Kato (1965), Hart & Lang (1965) and others.

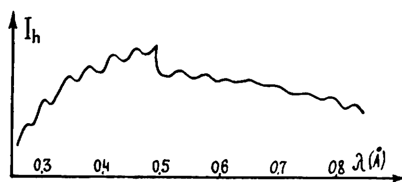

Fig. 4. Density distribution on a topograph in the direction of increasing wavelength. Photometering was carried out on the topograph of which a fraction is shown in Fig. 2(*a*).

The value of Λ_x was measured from a topograph, shown in Fig. 2(*a*), from five fringes over the wavelength range from 0·3 to 0·6 Å. The atomic scattering factor was calculated as $f_{111} = (4\sqrt{2})^{-1}F_{111}$ by substituting the value of Λ_x into (3). It was found to be $10{\cdot}69 \pm 0{\cdot}15$, which is in agreement with the results of measurements of other authors; *e.g.* Tanemura & Kato (1972) report the value of $f_{111} = 10{\cdot}66 \pm 0{\cdot}01$.

It should be mentioned that the accuracy of determination of the atomic scattering factor from topographs recorded with a continuous spectrum, can be improved, since about 20–30 fringes can be obtained from thick crystals. Precise measurements of $f_{\mathbf{h}}$ can be performed on plane-parallel wafers only over the ranges of λ values, far from absorption edges, where $f_{\mathbf{h}}$ is practically independent of the wavelength.

5. Dynamical contrast of topographs from wedge-shaped crystals

We now turn to the investigation of a more complicated contrast of topographs obtained from wedge-shaped crystal wafers, the thickness t of which varies evenly in the azimuthal direction **OY** (the wavelength in this direction remains constant). In this case one can expect that the intensity oscillations are observed both in the direction of the variation of wavelength and in that of the crystal thickness. The latter are similar to the integral intensity oscillations of transverse patterns with monochromatic radiation (Kato & Lang, 1959; Kato, 1961).

So, let $t = t_0 - m_y^{-1} y \tan \alpha$; here t_0 is the crystal thickness at the base of the wedge and α is the angle of the wedge. In this case the parameter A varies both in the radial (λ varies) and in the azimuthal direction (t varies). The period of oscillations of polychromatic integral intensity in the radial direction is determined as before by (3). In the azimuthal direction, the fringe spacing Λ_y is easily found from (2.1) by substituting in the expression for t:

$$\Lambda_y = m_y \cos \theta(\varrho_{2l+1} - \varrho_{2l-1})/KC|\chi_{\mathbf{h}}| \tan \alpha\,. \qquad (5)$$

Far from the element absorption edge $|\chi_{\mathbf{h}}|/\lambda^2$ is constant, so the constant intensity lines are hyperbolic curves $\lambda t/\cos\theta = \text{constant}$.

Fig. 5 shows a photograph of the topograph, obtained with continuous radiation, of a wedge-shaped Si wafer in the arrangement of Fig. 1 (reflexion 220, wedge angle $\alpha = 3°\,12'$). On the topograph are seen the lines Ag $K\alpha$ and Ag $K\beta$ of the characteristic radiation. The topograph was recorded with a voltage on the tube of 45 kV, therefore for $\lambda > 0{\cdot}6$ Å the 440 reflexion overlaps 220. A weak characteristic line is noticeable in the right-hand side of the topograph. This is the Ag $K\beta_1$ line of the 440 reflexion. The variation of integral inten-

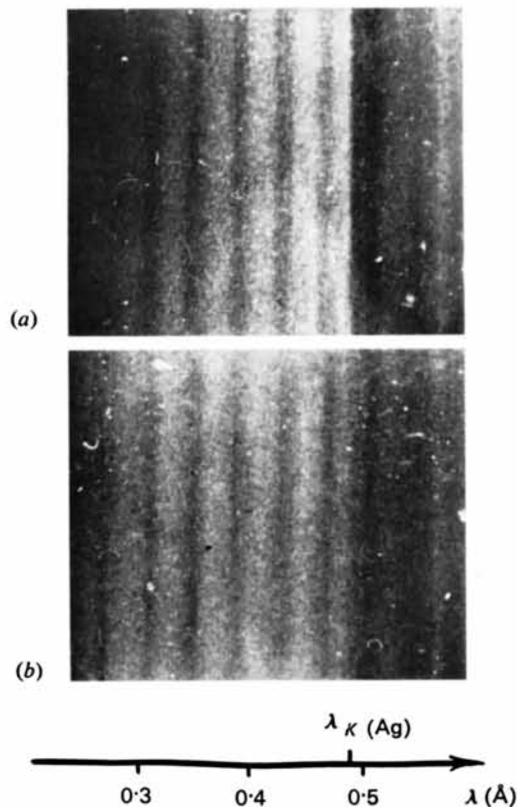

Fig. 2. Topographic image of a plane parallel Si single-crystal wafer 0.74 mm thick with continuous radiation: (*a*) crystal fixed during exposure, (*b*) crystal scanned during exposure (film in a fixed position). Photographic contrast of the photograph is opposite to that of the topograph.

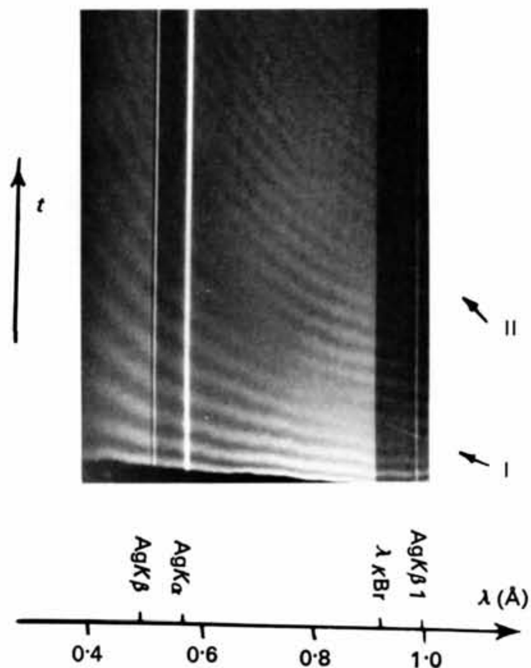

Fig. 5. A topograph of a wedged silicon wafer in continuous radiation. λ_K(Br) and λ_K(Ag) correspond to film sensitivity jumps at the *K* absorption edges of Br and Ag, and are equal to 0.92 and 0.48 Å respectively. The symbols I and II denote the areas where contrast starts to vanish.

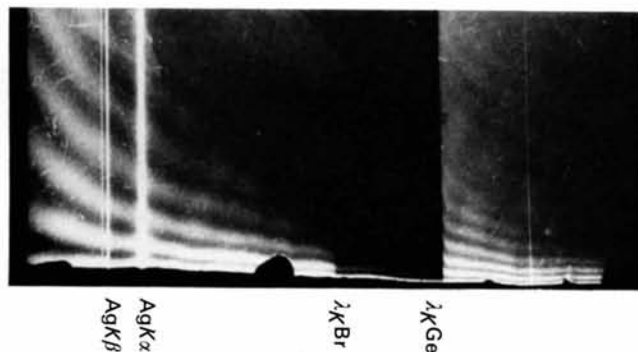

Fig. 7. A topograph of a wedged Ge wafer. λ_K(Ge) corresponds to the *K* absorption edge of Ge, λ_K(Ge) = 1.116 Å.

sity, corresponding to 440, is observed along this line. The superposition of 440 over 220 leaves the contrast of the 220 fringes on the topograph practically unaltered, since the intensity of the 440 reflexion is approximately six times weaker than that of 220.

As could be expected, the interference fringes are hyperbolically curved. The fringe spacing diminishes with increasing wavelength, because of the decrease of extinction length as λ increases. Two bands of low contrast, running at an angle to the constant intensity lines, are clearly seen on the topograph. It can again be assumed that the fading of contrast can be explained by the fact that the X-ray radiation comprises two states of polarization which lead to two periods of oscillation. Indeed, calculations show that lines of contrast fading due to the superposition of two systems of interference fringes must be of the form $t\lambda^3/\cos\theta = (N+\frac{1}{2}) \times \text{constant}$ (here $N=0,1,2\ldots$), which corresponds to the curves observed on the topographs. When the band of low contrast is passed, the fringe contrast becomes opposite, and the lines of constant intensity on a topograph on the opposite sides of the band of fading contrast form specific 'forks'.

All this confirms the hypothesis that the fading of contrast on topographs is caused by the superposition of two quasiperiodic functions $I_{\mathbf{h}}(x,y)$ for two states of polarization. As stated above, the superposition of two oscillations with closely spaced periods leads not only to lowering the contrast of interference patterns when oscillations superpose in opposite phases, but also to modification of the period observed. This must be taken into account when $f_{\mathbf{h}}$ is measured. Namely, (5) yields a correct value of Λ_y in the areas not directly adjacent to that of contrast fading, if the quantity $0{\cdot}5(1+|\cos 2\theta|)$ is taken to be the polarization factor.

Thus, the interference picture in the case discussed varies in the directions of change of both wavelength and crystal thickness. This makes it possible to offer a method of determining the dependence of the atomic scattering function on wavelength.

6. Measurement of the dependence of the atomic scattering function on wavelength

(*a*) *Silicon, reflexion* 220

We have measured Λ_y on a topograph, shown in Fig. 5, at an interval of $\Delta\lambda = 0{\cdot}05$ Å. The measured values of Λ_y were substituted into (5) and $f_{\mathbf{h}}$ was then calculated. In Fig. 6 are represented the experimental values $f_{\mathbf{h}}(\lambda)$. At the points $\lambda = 0{\cdot}468$ and $\lambda = 0{\cdot}886$ Å errors are indicated in finding $f_{\mathbf{h}}$ for short- and long-wavelength portions of the graph $f_{\mathbf{h}}(\lambda)$. Errors in determining the wavelength at any point of the topograph are not greater than 5×10^{-4} Å. Crosses on the plot mark the values of $f_{\mathbf{h}}$ taken from the paper by Hart & Milne (1969) for $\lambda = 0{\cdot}559$ Å (Ag $K\alpha_1$) and $\lambda = 0{\cdot}709$ Å (Mo $K\alpha_1$). The solid line in Fig. 6 plots the theoretical dependence $f_{\mathbf{h}}(\lambda)$, corrected for thermal motion. The values of $f_{\mathbf{h}}$ and the Debye–Waller factor $\exp(-M)$ at 20°C were taken from *International Tables for X-ray Crystallography* (1962), dispersion corrections were calculated according to Hönl's theory (James, 1948).* We see that, within measurement errors, the experimental points fit the theoretical curve $f_{\mathbf{h}}(\lambda)$.

In our experiments, the accuracy of determining $f_{\mathbf{h}}$ is restricted by that of the wedge preparation and by that of measuring the distance Λ_y. It should be noted that some authors have succeeded in the measurement of $f_{\mathbf{h}}$ for Si with monochromatic radiation to an accuracy of up to 0·1 % (see, for example, Hart & Milne, 1969; Tanemura & Kato, 1972). Such high accuracy appears to be feasible also for measuring $f_{\mathbf{h}}$ from interference fringes, obtained in polychromatic radiation. However, the present investigation was aimed at demonstrating the principal possibility of measuring the dependence $f_{\mathbf{h}}(\lambda)$, so we have restricted ourselves to the accuracy mentioned above.

(*b*) *Germanium, reflexion* 111

The dependence $f_{\mathbf{h}}(\lambda)$, measured in Si, is a straight line running at a small angle to the λ axis, because the range of wavelength for which the graph is plotted lies far from the K absorption edge [$\lambda_K(\text{Si}) = 6{\cdot}74$ Å]. Measurements of $f_{\mathbf{h}}(\lambda)$ in a narrow wavelength interval close to the absorption edges of the element are of special interest, since the theoretical methods of calculating dispersion corrections do not allow one to calculate the values of $\Delta f'$ and $\Delta f''$ in this region with the reliability and accuracy desired. At the same time, the experimental measurements carried out up to the present, close to the absorption edges of elements, have run into a number of difficulties and are not sufficiently accurate.

The method suggested makes it possible to study in much detail the behaviour of the function $f_{\mathbf{h}}(\lambda)$ close to the absorption edges of elements of which high-perfection single crystals can be grown. Fig. 7 gives an example of a topograph recorded with continuous X-ray radiation of a wedged Ge wafer by means of the set-up given in Fig. 1: 111 reflexion; the wedge angle was approximately 1°20′. On the topograph are shown the lines of characteristic radiation of the silver anode. In

* According to James, $f_{\mathbf{h}}(\lambda) = f_{\mathbf{h}0} + \Delta f'(\lambda) + i\Delta f''(\lambda)$, where $f_{\mathbf{h}0}$ corresponds to the scattering with wavelength much shorter than the absorption edge and $\Delta f'$ and $\Delta f''$ are dispersion corrections.

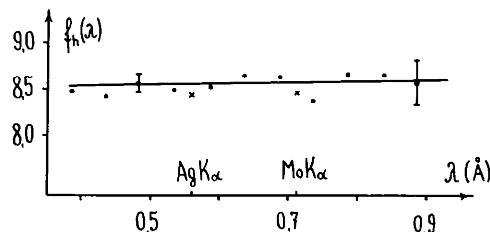

Fig. 6. Atomic scattering factor $f_{\mathbf{h}}$ as function of X-ray wavelength; Si, 220 reflexion.

the long-wavelength portion of the topograph the 111 reflexion is overlapped by 333. This reflexion is much weaker than 111, and we can assume that the contrast of interference fringes on the topograph is mainly determined by the 111 reflexion.* As in the topograph for a Si crystal, we see a fringe of low contrast due to the presence of two polarization states in the X-ray radiation. Both the contrast and the number of interference fringes observed depend on the absorption coefficient μ. For $\lambda > \lambda_K$, μ is not large, and the topograph reveals up to 15 polychromatic interference fringes in the azimuthal direction. For $\lambda < \lambda_K$ the linear absorption coefficient reaches $\sim 10^3$ cm^{-1} at the extinction length of about 10 μm, so that in this region the number of fringes decreases to 2–3. Not only the visibility of the fringes but also their shape changes close to the absorption edge. Fringes are curved, and this bend is seen both to the right and to the left of λ_K. The direction of curvature indicates that close to λ_K the extinction length increases, *i.e.* f_h diminishes.

The interference fringe spacings were measured on the topograph shown in Fig. 7. Measurements were performed close to λ_K by two fringes at $\lambda < \lambda_K$ and by four fringes for $\lambda > \lambda_K$. The measurement accuracy was 6–8 % and 3–4 % respectively. Calculations were made by means of (5). Rigorously speaking, (5) can be used only for low-absorption crystals, since it gives somewhat overestimated values (see Kshevetskii, Mikhailyuk & Ostapovich, 1975). In a high-absorption crystal the fringe spacing is determined by a more complicated function of t and λ. However, Kato's (1968) results indicate that the change of spacings Λ_y of visible interference fringes due to the absorption for $\mu t < 3$ is smaller than our experimental accuracy and thus we can use (5) for the whole range of wavelengths.

In order to calculate the dependence $f_h(\lambda)$ and to compare it with the theoretical results, it was necessary to measure accurately the wedge angle. Wedges with the required values of the angle α and acute edge thickness less than 10 μm are usually nonuniform; the acute edges of the wedges are apt to round-off because of etching. Batterman & Patel (1968) ran into similar difficulties in preparing Ge wedges. We needed to know the wedge angle α in a sufficiently narrow region of the crystal where the radiation with $\lambda \sim \lambda_K$ is diffracted. In this narrow region the angle of the wedge can be considered constant. We assumed that the experimental and theoretical values of f_h coincide for $\lambda/\lambda_K = 1{\cdot}2$. (This assumption is based on the measurements of f_h with monochromatic radiation, far from absorption edges.) Having measured Λ_y for $\lambda/\lambda_K = 1{\cdot}2$, we calculated the value of α by means of (5). This value of the wedge angle was used for calculating $f_h(\lambda)$ for all other values of λ.

In Fig. 8 solid circles mark experimental points of the function $\delta f_h = f_h - f_{h0}$. Experimental errors are indicated for $\lambda \simeq 1{\cdot}30$ and $\lambda \simeq 1{\cdot}03$ Å for points with $\lambda > \lambda_K$ and $\lambda < \lambda_K$, respectively. The solid line on the graph plots the dependence $\delta f_h(\lambda/\lambda_K) = \Delta f' + (\Delta f'')^2 / 2(f_{h0} + \Delta f')$, where $\Delta f'$ and $\Delta f''$ are calculated from Hönl's theory (James, 1948), and f_{h0} was assumed to equal 27·4.

Within the experimental errors, the experimental points coincide with the theoretical curve. The experimental dependence obtained confirms the known behaviour of the atomic scattering function close to the Ge K absorption edge.

Note that the accuracy of measurement obtained in our experiments is likely to be improved with the application of more complicated experimental procedures and by more precise allowance made for all parameters affecting the value Λ_y. This is demonstrated by the experimental results obtained by Batterman & Patel (1968) who have measured the atomic scattering factor of Ge, with the radiation Ag $K\alpha$, to within 1 %.

Conclusion

The quasiperiodic variation of intensity arises on topographs under the diffraction of continuous radiation both on plane-parallel and wedge-shaped wafers of perfect crystals. The intensity oscillations observed are the polychromatic *Pendellösung* fringes. In measuring the fringe spacing, Λ_x, one can determine the value of the atomic scattering factor of the perfect plane-parallel crystals as well as those with small dimensions [(such crystals should be scanned during exposure on a fixed film as in the case of obtaining the topograph given in Fig. 2(*b*)]. By applying the wedge-shaped crystals, one can determine experimentally the dependence of the atomic scattering factor on the wavelength. This possibility is of special interest for the wavelengths close to the element absorption edges where the method described makes it possible to trace the whole run of the curve $f_h(\lambda)$.

The present paper discusses one of the possible applications of polychromatic interference fringes. We believe that diffraction of continuous radiation will prove to be useful for the investigation of many-wave diffraction in X-ray interferometry [the conditions

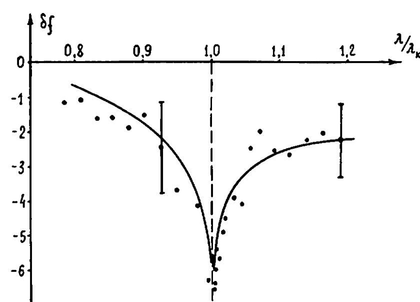

Fig. 8. Anomalous dependence of $\delta f_h = f_h - f_{h0}$ on X-ray wavelength close to the Ge K absorption edge.

* No superposition of the two reflexions is produced in the range $\lambda < \lambda_K$, since the topograph was reported at an X-ray tube voltage of 34 kV.

under which moiré fringes are observed in the X-ray interferometer with continuous radiation are similar to those obtained by Bonse & te-Kaat (1971) for moiré fringes with monochromatic radiation from an extended source (Shulakov & Aristov, 1976)].

The next paper will be devoted to a detailed analysis of the experimental arrangement on the basis of the spherical-wave approximation of diffraction (Kato, 1961) and to the derivation of the dependence of the observed variations of intensity on the experimental geometry and on the dynamical characteristics of the crystal.

References

ARISTOV, V. V., SHMYTKO, I. M. & SHULAKOV, E. V. (1976*a*). Abs. of Rep. 4th All-Union Conf. Dynamical Effects of the Scattering of X-rays and Electrons, 31 March–2 April, Leningrad, p. 11.
ARISTOV, V. V., SHMYTKO, I. M. & SHULAKOV, E. V. (1976*b*). *Kristallografiya*, **21**, 351–356.
ARISTOV, V. V., SHMYTKO, I. M. & SHULAKOV, E. V. (1977). *Acta Cryst.* A**33**, 418–423.
ARISTOV, V. V. & SHULAKOV, E. V. (1975). *J. Appl. Cryst.* **8**, 445–451.
AUTHIER, A. & SIMON, D. (1968). *Acta Cryst.* A**24**, 517–526.
BATTERMAN, B. W. & PATEL, J. R. (1968). *J. Appl. Phys.* **39**, 1882–1887.
BONSE, U. & TE-KAAT, E. (1971). *Z. Phys.* **243**, 14–45.
FUKAMACHI, T. & HOSOYA, S. (1975). *Acta Cryst.* A**31**, 215–220.
HART, M. & LANG, A. R. (1965). *Acta Cryst.* **19**, 73–77.
HART, M. & MILNE, A. D. (1969). *Acta Cryst.* A**25**, 134–138.
HASHIMOTO, H., KOZAKI, S. & OHKAWA, T. (1965). *Appl. Phys. Lett.* **6**, 16–17.
HATTORI, H., KURIYAMA, H. & KATO, N. (1965). *J. Phys. Soc. Japan*, **20**, 1047–1050.
INDENBOM, V. L. & CHUKHOVSKII, F. N. (1972). *Usp. Fiz. Nauk*. **107**, 229–265.
International Tables for X-ray Crystallography (1962). Vol. III. Birmingham: Kynoch Press.
JAMES, R. W. (1948). *The Optical Principles of the Diffraction of X-Rays*, London: Bell.
KATO, N. (1961). *Acta Cryst.* **14**, 627–636.
KATO, N. (1968). *J. Appl. Phys.* **39**, 2225–2230, 2231–2237.
KATO, N. (1969). *Acta Cryst.* A**25**, 119–128.
KATO, N. & LANG, A. R. (1959). *Acta Cryst.* **12**, 787–794.
KOZAKI, S., OHKAWA, T. & HASHIMOTO, H. (1968). *J. Appl. Phys.* **39**, 3967–3976.
KSHEVETSKII, S. A., MIKHAILYUK, I. M. & OSTAPOVICH, M. V. (1975). *Ukr. Fiz. J.* **20**, 610–615.
PINSKER, Z. G. (1974). *Dynamical Scattering of X-rays in Ideal Crystals*. Moscow: Nauka.
SHULAKOV, E. V. & ARISTOV, V. V. (1976). Abs. Rep. 4th All-Union Conference on Dynamical Effects of the Scattering of X-rays and Electrons. 31 March–2 April, Leningrad, pp. 57–58.
TANEMURA, S. & KATO, N. (1972). *Acta Cryst.* A**28**, 69–80.
WALLER, I. (1926). *Ann. Phys.* **79**, 261–273.
ZACHARIASEN, W. H. (1945). *Theory of X-ray Diffraction in Crystals*. New York: John Wiley.

Acta Cryst. (1977). A**33**, 418–423

Dynamical Contrast of the Topographic Image of a Crystal with Continuous X-ray Radiation. II. A Theoretical Study of the Polychromatic Interference Fringes*

BY V. V. ARISTOV, I. M. SHMYTKO AND E. V. SHULAKOV

Solid State Physics Institute, Academy of Sciences of the USSR, Moskovskaya Oblast, Chernogolovska, 142432, *USSR*

(*Received* 31 *March* 1976; *accepted* 13 *December* 1976)

A theoretical analysis is given of the contrast of the topographic image of a perfect crystal with continuous radiation. Conditions for observation of polychromatic interference fringes in this diffraction scheme are analysed on the basis of Kato's dynamical theory of spherical-wave diffraction. The effect of polarization and azimuthal divergence of X-rays on the contrast of topographs is also discussed.

1. Introduction

In the preceding paper (Part I: Aristov, Shmytko & Shulakov, 1977) we have reported the experimental investigation of the contrast on topographical images obtained for perfect single-crystal Si and Ge wafers in a set-up with a point source of divergent continuous X-ray radiation. It was demonstrated that topographs display polychromatic interference fringes.

In the present paper we apply the dynamical theory of spherical-wave diffraction by perfect crystals (Kato, 1961*a*, *b*) to the analysis of contrast on the topographs of perfect crystals, produced by continuous X-ray radiation. The analysis is restricted to the case of symmetric Laue diffraction by the crystal with zero absorption. This approximation enables one to derive simple expressions for the intensity of diffracted radia-

* Copyright reserved by the All-Union Agency on Authors' Rights.